



Monitoring marine heatwaves in Salvador-BA using SiMCosta data

Bruna Alves Oliveira Destéfani^{2*}, Carlos Alberto Eiras Garcia^{1,2}

¹ Centro de Estudos dos Oceanos e Clima – Instituto de Oceanografia – Universidade Federal do Rio Grande (Rio Grande - Av. Itália Km 08, sn, 96.203-900 – RS – Brazil).

² Sistema de Monitoramento da Costa Brasileira (SiMCosta) – Centro de Estudos dos Oceanos e Clima – Instituto de Oceanografia – Universidade Federal do Rio Grande (Rio Grande - Av. Itália Km 08, sn, 96.203-900 – RS – Brazil).

* Corresponding author: bruna.simcosta@gmail.com

ABSTRACT

The frequency, duration, and intensity of Marine Heatwaves (MHWs) have been increasing, with a notable trend in the South Atlantic. This study investigates MHW occurrences over the past five years (August 2019 to April 2024) using sea surface temperature (SST) data from the Tracker tool and the SiMCosta BA01 buoy, located in Salvador, Bahia, Brazil. The Tracker identified 23 MHW events, while the SiMCosta buoy revealed 42 events, indicating greater variability due to local dynamics. A particularly significant event occurred in March 2024, with a maximum SST anomaly of 2.61°C. The onset of this warming coincided with an extreme El Niño in the Tropical Pacific, suggesting a possible interaction between global climate patterns and local extremes. The identification and analysis of MHW events using the SiMCosta buoy highlight the need for continuous and detailed monitoring of meteorological and oceanographic data to better assess and understand local climatic extremes and their impacts, especially on marine ecosystems and regional economic activities.

Keywords: Sea surface temperature anomalies, Local climate extremes, Ocean observation

Marine heatwaves (MHWs) are extreme ocean temperature events with significant ecological, climatic, and socioeconomic impacts. They occur during prolonged periods of abnormally high sea surface temperatures and have become more frequent, intense, and persistent in recent decades due to anthropogenic climate change. According to Oliver et al. (2018), factors such as atmospheric heatwaves, ocean currents, and climate oscillations like El Niño can trigger these events. Ecologically, MHWs can cause severe stress to marine ecosystems, leading to

widespread coral bleaching, as observed during the 2016 Great Barrier Reef event (Hughes et al., 2018; Morgan et al., 2017) and during March and April 2019 in the Abrolhos Bank (16°40'–19°40'S, 39°10'–37°20'W), the largest and richest coral reefs in the South Atlantic (Ferreira et al., 2021), when elevated temperatures caused significant coral mortality. Additionally, MHWs alter life cycles and distribution of marine species, disrupting predator-prey dynamics and potentially leading to fishery collapses. Prolonged heatwaves can cause loss of kelp forests and seagrass meadows, degrading critical habitats that support a wide variety of marine life.

Economically, MHWs directly impact fisheries (Cheung and Frölicher, 2020) and tourism (González Hernández et al., 2023), affecting regions dependent on marine resources. These

Submitted: 16-Sep-2024

Approved: 15-Apr-2025

Editor: Rubens Lopes



© 2025 The authors. This is an open access article distributed under the terms of the Creative Commons license.

impacts can lead to declines in fish stocks, affecting food security and livelihoods. For example, the 2014-2016 'Blob' event in the Northeast Pacific caused significant economic losses in the commercial fishing industry due to changes in fish populations (Yang et al., 2019) and the occurrence of harmful algal blooms (Roberts et al., 2019). Smith et al. (2021) explored the effects of MHWs globally, highlighting that the economic impact of some isolated MHW events resulted in direct losses exceeding \$800 million and indirect losses of up to \$3.1 billion in ecosystem services over several years. Thus, MHWs have led to harmful algal blooms, mass mortality events, and profound transformations in entire ecosystems, affecting habitats, regulation, and global ecosystem services.

Broadly, MHWs influence climate patterns and the global climate system. They intensify atmospheric heatwaves and affect precipitation patterns, contributing to extreme weather events on land. The interconnectedness of marine and atmospheric systems makes MHWs crucial in climate variability, whose understanding is essential to effectively predict and mitigate future climate impacts. Researchers have identified a significant increase in the frequency, duration, and intensity of MHWs globally (Oliver et al., 2018), and Costa and Rodrigues (2021) found a rising trend in the South Atlantic.

In this study, we investigated MHWs using climatological data from the Tracker tool (Schlegel, 2020) and daily sea surface temperature (SST) data collected by the Brazilian Coastal Monitoring System (SiMCosta) BA01 buoy, located in Salvador, Bahia (Brazil), over the past five years. The website marineheatwaves.org provided MHW climatology information free of charge, while the SiMCosta distributed the in situ SST data. We focused on the occurrence of MHWs between August 2019 and April 2024 in the Salvador region.

The SiMCosta BA01 buoy, model WatchKeeper (AXYS Technologies), measures the following meteo-oceanographic parameters: wind intensity and direction, air temperature, atmospheric pressure, total solar radiation, wave height and direction, coastal current intensity and direction, water temperature (SST), salinity, turbidity, dissolved oxygen, and chlorophyll concentration. The SST

sensor is the Seabird Microcat SBE37-SMP-ODO, positioned at a depth of approximately 1 m. The maintenance team cleans the sensors about every 30 days. The equipment takes measurements every half hour and undergoes regular calibration.

Regarding MHWs, we used the definition by Hobday et al. (2016), which considers an abnormally warm event as an MHW if it lasts five or more days, with temperatures above the 90th percentile, considering historical climatology (provided by marineheatwaves.org). The NOAA OISST database was the basis for the climatology calculated by the Tracker. To enhance the climatology applied to the buoy data, we calculated the correlation and linear regression between NOAA OISST and SiMCosta BA01 buoy data over a simultaneous three-year period (2019-2022). Since the buoy lacks a 30-year data record for establishing its own climatology, this approach enabled us to develop a more accurate climatology. We observed a strong correlation between datasets ($r = 0.9$, $p < 0.05$, $n = 1096$, bias = 0.011°C). We extracted and analyzed the anomalies from the three-year period series and found a good correlation ($r = 0.53$, $p < 0.05$, $n = 1096$, bias = $-2 \times 10^{-16}^{\circ}\text{C}$). Then, we used linear regression to adjust the OISST anomaly series and align it with the buoy anomaly series from SiMCosta BA-01. As a result, it was possible to transform the NOAA OISST climatology series by applying the derived linear equation between the adjusted SST NOAA OISST series and the SST SiMCosta BA-01 series. This yielded a high correlation ($r = 0.92$, $p < 0.05$, $n = 1096$, bias = $8 \times 10^{-18}^{\circ}\text{C}$), demonstrating that the climatology approach employed in this study is robust and reliable.

Each MHW event has specific attributes defined by Hobday et al. (2016): duration (consecutive period during which the temperature exceeds the threshold), maximum intensity (highest anomaly value during the MHW), mean intensity (average temperature anomaly during the MHW), and cumulative intensity (sum of daily intensity anomalies during the MHW). Annual frequency refers to the count of events in a given year. This study also used the MHW severity categories, a method proposed by Hobday et al. (2018), to classify each MHW identified in the study region.

Finally, air-sea heat fluxes were calculated based on Fairall et al. (1996), as implemented in the COARE 3.0 model version. The sensible heat flux (Q_H), defined as the heat transferred due to the temperature difference between the ocean surface and the air immediately above, is calculated using:

$$Q_H = \rho \cdot cp \cdot C_H \cdot U \cdot (T_s - T_a)$$

where ρ is the air density (approximately 1.2 kg.m^{-3}), cp is the specific air heat capacity (approximately 1004 J/(kg.K)), C_H is the sensible heat transfer coefficient (a typical value is around 1.2×10^{-3}), U is the wind speed at a specific height above the surface (in m.s^{-1}), T_s is the sea surface temperature ($^{\circ}\text{C}$), and T_a is the near-surface air temperature ($^{\circ}\text{C}$). The Latent Heat Flux (Q_E) is defined as the heat transferred due to water evaporation or condensation at the ocean-atmosphere interface. It is calculated using:

$$Q_E = \rho \cdot Lv \cdot C_E \cdot U \cdot (q_s - q_a)$$

where ρ is the air density, Lv is the latent heat of vaporization of water (approximately $2.5 \times 10^6 \text{ J.kg}^{-1}$), C_E is the latent heat transfer coefficient (a typical value is around 1.2×10^{-3}), U is the wind speed at a specific height above the surface, q_s is the specific humidity at the sea surface, and q_a is the specific humidity of the near-surface air.

Data from the meteo-oceanographic buoy also helped calculate the shortwave liquid flux (Q_{sw}) and longwave liquid flux (Q_{Lw}), as well as the heat balance (Q_{net}):

$$Q_{sw} = R \cdot (1 - \alpha)$$

where R is the incident solar radiation and α is the surface albedo (a typical value for water is 0.055). QLW is estimated using the Clark et al. (1974) bulk formula (Fung et al., 1984):

$$Q_{Lw} = \epsilon \sigma T_s^4 (0.39 - 0.05 e_a^{1/2}) (1 - 0.51 C^2) + 4 \epsilon \sigma T_s^3 (T_s - T_a)$$

where σ is the Stefan–Boltzmann constant ($5.67 \times 10^{-8} \text{ W/m}^2 \times \text{K}^4$), ϵ is the surface emissivity (a typical value for water is 0.97), T_s is the sea surface temperature in Kelvin, T_a is the air

temperature in Kelvin, e_a is the vapor pressure near the surface (calculated using the Tetens equation), and C is the cloud cover index (which ranges from 0 [clear sky] to 1 [overcast sky]). C is estimated by inverting the expression from Reed (1977):

$$C = 1.61(1 - Q_{sw} / Q_{cs} + 0.0019n)$$

where Q_{cs} is the clear-sky radiation (Ångström–Prescott equation) and n is the solar altitude at noon.

Finally, the heat balance Q_{net} at the ocean-atmosphere interface (Hsiung, 1985):

$$Q_{net} = Q_{sw} + Q_{Lw} + Q_H + Q_E$$

The buoy time series provides data every half hour. For daily analysis, data around 2:00 PM were selected, as the shortwave liquid flux depends on solar radiation, which is absent at night.

Between August 2019 and April 2024, we identified 49 MHW events in the SST data measured by the SiMCosta BA01 buoy (Table 1). The Tracker tool identified 23 MHW events in the same period and region as the buoy. The greater variability in the high-frequency data measured by the buoy and the complexity of local dynamics justify this difference. Between July and November 2023, the Tracker tool detected an MHW event lasting 115 days. During this period, the SST data from the buoy recorded six events, totaling 87 days. This indicates that the MHW identified in the Tracker database also appears in the SiMCosta data, but with greater variability in the latter. This highlights the need for a continuous series of meteo-oceanographic data, which captures the complexity and real conditions of the region, thereby validating climate outcomes. Additionally, this data series becomes a crucial tool for detecting local climate change or abrupt events.

In the analyzed years, the period between September and November recorded the highest incidence of MHWs in Salvador (Figure 1). A continuous warming event was notable between September 2023 and April 2024, when the Tracker and buoy data classified the MHWs as strong. Between March 19 and 21, 2024, data from the buoy identified severe warming, with a

maximum anomaly of 2.61°C (Figure 1E). This warming coincides with the extreme El Niño event in the Tropical Pacific, which occurred between November 2023 and January 2024.

Table 1. Characteristics of MHWs identified by the Tracker tool and the SiMCosta BA01 buoy data. Data for 2019 were analyzed as of August (*). Data for 2024 were analyzed up to April (**).

year	method	events n°	duration (days)	intensity mean (°C)	intensity max (°C)	cumulative (°C)
2019*	Tracker	5	122	0.93	1.5	127.78
	SiMCosta	9	91	0.86	1.80	85.33
2020	Tracker	7	106	0.85	1.17	92.38
	SiMCosta	9	119	0.93	1.83	114.18
2021	Tracker	2	49	0.82	1.24	44.72
	SiMCosta	4	81	1.06	1.77	86.29
2022	Tracker	3	63	0.85	1.07	54.83
	SiMCosta	6	76	0.99	1.79	74.44
2023	Tracker	4	199	0.88	1.59	185.83
	SiMCosta	15	169	0.93	1.73	166.26
2024**	Tracker	2	84	1.15	1.72	104.18
	SiMCosta	6	83	1.17	2.61	99.72

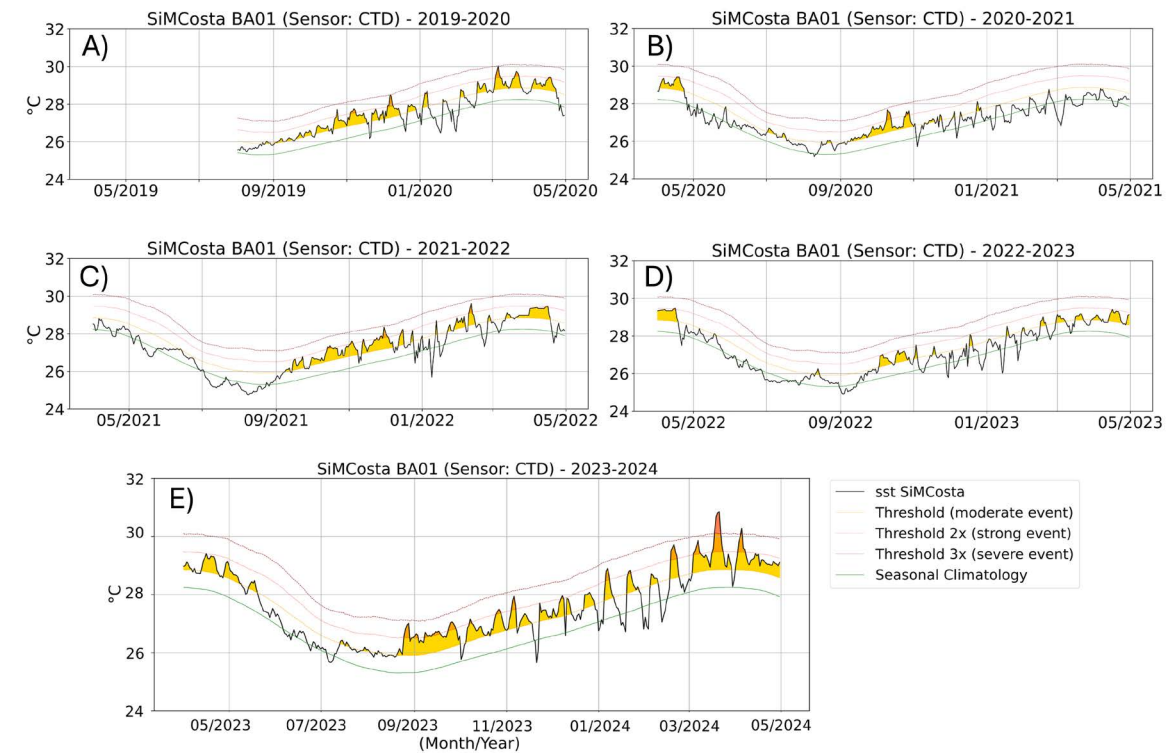


Figure 1. SST time series and identification of MHWs with seasonal climatology. A) Period between 2019 and 2020. B) Period between 2020 and 2021. C) Period between 2021 and 2022. D) Period between 2022 and 2023. E) Period between 2023 and 2024.

El Niño and the Southern Oscillation (ENSO) significantly alter global atmospheric circulation (Garfinkel and Hartmann, 2010; Hoerling et al., 1997; Neelin et al., 2003), affecting Hadley (HC) and Walker cells and causing climatic fluctuations in the tropics and extratropics via atmospheric teleconnections (Taschetto et al., 2020). According to Oliver et al. (2018), El Niño generates long-lasting and high-intensity MHWs.

In South America, numerous studies explore changes caused by ENSO events (Cai et al., 2020; Grimm et al., 2000; Medeiros and Oliveira, 2021; Rodrigues et al., 2011; Rodrigues and McPhaden, 2014; Tedeschi, 2015). Recently, Li et al. (2023) examined the variability of HC triggered by ENSO events and identified a HC decrease in the Tropical Atlantic Ocean during El Niño events, which affects trade winds in the area. Furthermore, Rodrigues and McPhaden (2014) demonstrated that, in northeastern Brazil, the SST meridional gradient is crucial in determining the position of the Intertropical Convergence Zone (ITCZ)—a region known for intense cloud formation. Positive SST anomalies in the Tropical Atlantic weaken the southeast trade winds, shift the ITCZ southward, and alter precipitation patterns in the region. Giannini et al. (2004) highlight that the weakening of trade winds reduces vertical mixing of water and raises SST. Discussions suggest that one factor drives the other, establishing a cycle that perpetuates SST warming and trade wind weakening for a certain period, which can favor MHW events.

The Atlantic Meridional Mode (AMM) represents a climate variability pattern in the Tropical Atlantic, identified with maximum covariance analyses between SST and the zonal and meridional components of the 10-meter wind field (Chiang and Vimont, 2004). This approach detects co-variation patterns between SST and surface winds in the region. The AMM directly influences the dynamics of the ITCZ, modifying rainfall distribution and atmospheric circulation patterns in the Tropical Atlantic.

The AMM generates an anomalous SST gradient, shifting the ITCZ toward the warmer hemisphere, where SST is higher (Nobre and Shukla, 1996). During the positive phase of the AMM, the ITCZ moves northward, leading to drought conditions in northeastern Brazil. Additionally,

warmer-than-normal SST and weaker vertical wind shear during this phase favor the formation and intensification of tropical cyclones in the Atlantic (Foltz et al., 2012).

The canonical El Niño phenomenon also is key in warming the Tropical Atlantic (Amaya and Foltz, 2014). Figure 2A shows that the severe MHW event in March 2024 occurred when both the AMM and El Niño 3.4 indices were positive. This combination significantly alters atmospheric circulation patterns, reduces rainfall, and decreases moisture transport from the South Atlantic, leading to droughts in the Amazon Basin and northeastern Brazil (Drumond et al., 2014).

The maps in Figure 2B display SST anomalies, wind speed, relative humidity, and total cloud cover from the ERA5 reanalysis for March 2023 and March 2024. It is evident that SST shows positive anomalies throughout the Tropical Atlantic in March 2024, with values significantly higher than those observed in March 2023. Relative humidity also shows higher values in March 2024. Regarding wind speed and total cloud cover, the maps reveal decreased values in the study region between March 2023 and March 2024.

ERA5 reanalysis data from March 2024 show lower relative humidity in northeastern and southeastern Brazil compared to March 2023, while northern Brazil and regions near the equator recorded increased humidity, likely associated with ITCZ displacement. The reduced humidity in Bahia resulted in fewer clouds, enabling more solar radiation to reach the sea surface and warm the water (Figure 2A).

More recently, researchers reported that, in addition to the weakening of the HC and Walker cells, the Rossby wave train contributed to drier and less cloudy conditions during the 2015–2016 El Niño in northeastern Brazil (Medeiros and Oliveira, 2021). These observations reinforce that climate change, driven by global warming, is altering the way ENSO events affect atmospheric circulation. This suggests that ENSO-related teleconnections will become even more complex and unpredictable as the global climate continues to warm (Taschetto et al., 2020). Thus, it is crucial to focus on processes involving MHW events, considering their increasingly significant implications in the current climate scenario.

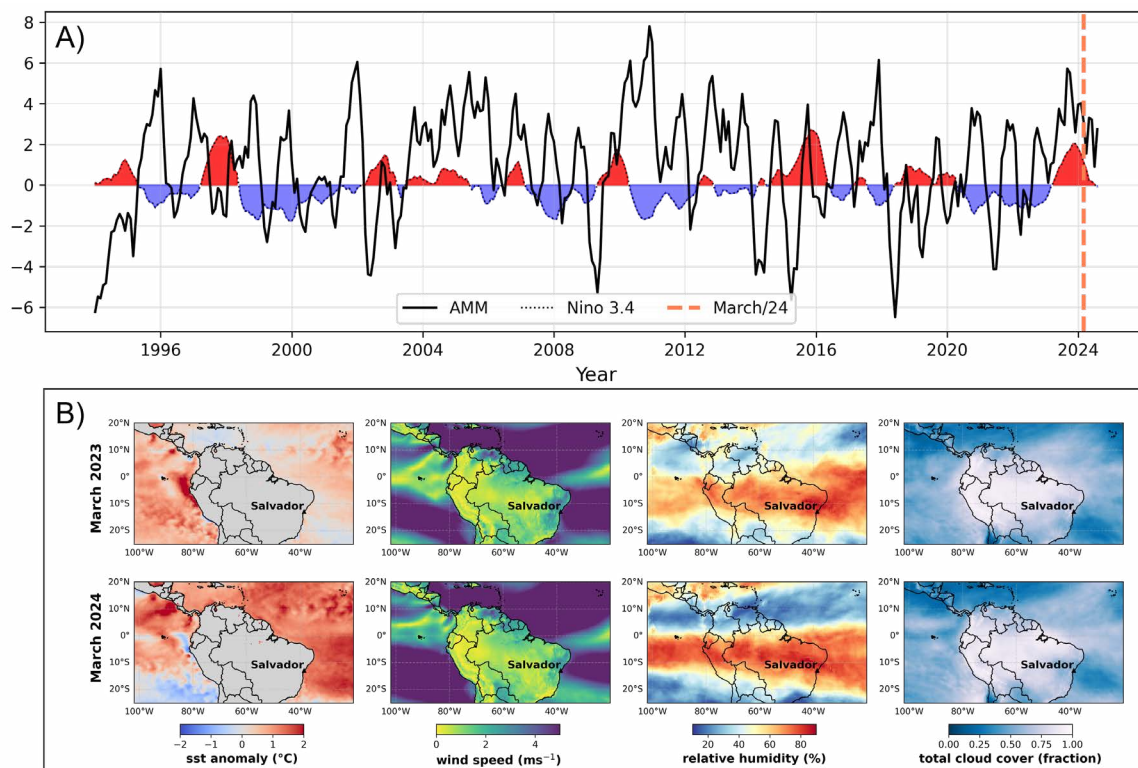


Figure 2. A) Climate indices AMM (Atlantic Meridional Mode) and Niño 3.4 (source: NOAA Physical Sciences Laboratory - <https://psl.noaa.gov/data/climateindices/list/>). B) Monthly average SST anomalies, wind speed, relative humidity, and total cloud cover from the ERA5 reanalysis for March 2023 and March 2024. The coral dotted line represents March 2024, marking the occurrence of a severe MHW event.

Data from the SiMCosta BA01 buoy in March 2024 revealed important meteorological and oceanographic characteristics during a severe MHW event. During this period, measurements recorded low wind speeds (Figure 3A), averaging less than 5 m.s^{-1} , indicating relatively calm atmospheric conditions, which reduce vertical water mixing and elevate SST. Further, the data show a significant drop in relative humidity (Figure 3B), suggesting the presence of drier air masses over the region monitored by the buoy.

Meteorological and oceanographic variables provided by the buoy made it possible to calculate sensible and latent heat fluxes, which are fundamental to understand energy exchange between the atmosphere and the ocean. As of January 2024, the sensible heat flux began to show negative values, indicating a heat transfer

from the atmosphere to the ocean. This suggests that the ocean consistently absorbed heat from the atmosphere for three months, contributing to the intensification of the MHW event in March. Figure 3 illustrates this dynamic. The data indicate that weakened winds and decreased humidity reduce evaporation and limit latent heat cooling, potentially contributing to SST increase. Under weak wind conditions, lower turbulence reduces heat exchange between the ocean surface and the atmosphere, while also restricting the mixing of surface water layers. This process inhibits the efficient dissipation of energy accumulated at the surface during the day through solar radiation, leading to higher SST. Decreased evaporation also results in less latent heat removal from the system, further enhancing surface warming. The graph shows a decline in latent heat flux (Figure 3F).

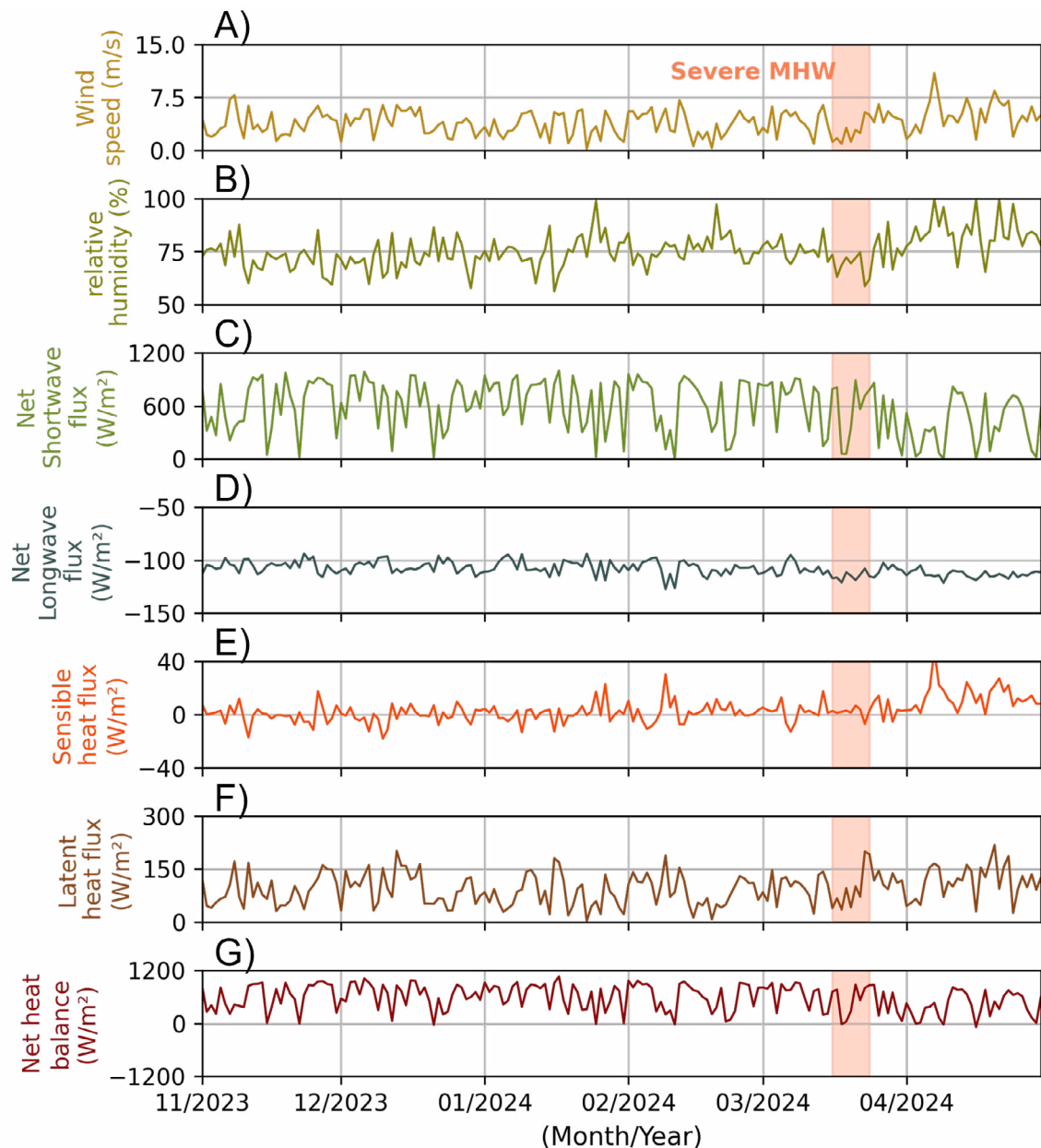


Figure 3. Time series at 2PM obtained from the SiMCosta BA01 buoy data between 11/2023 and 04/2024. A) wind speed, B) relative humidity, C) net shortwave, D) net longwave, E) sensible heat flux, F) latent heat flux, and G) net heat balance. The coral-colored shaded area represents the period when the severe MHW event occurred.

In the tropics, the drivers of MHW events differ from those in mid- and high-latitudes (Vogt et al., 2022). In this event, reduced heat exchange with the atmosphere and diminished evaporative cooling appear to be the primary contributors to SST increase, as shortwave radiation does not directly or significantly impact the warming observed during this period.

Vogt et al. (2022) described how reduced vertical diffusion initiates MHWs in the equatorial Pacific by preventing efficient heat transfer from the surface to deeper layers. In this process, weaker winds intensify water column stratification, increasing the temperature gradient between surface and deeper layers. Stronger stratification suppresses heat mixing and diffusion, limiting vertical heat transfer.

As a result, heat accumulates in the surface layers, driving excessive warming and the development of a MHW. A similar mechanism likely occurred during the severe MHW event observed in March 2024 by the SiMCosta BA01 buoy.

These analyses are corroborated by Oliver et al. (2018), who reported that MHWs frequently occur under high atmospheric pressure systems with reduced winds, which diminish vertical water mixing and may be accompanied by low latent heat loss, further increasing the temperature. These observations underscore the importance of monitoring air-sea interactions to better understand the mechanisms driving extreme ocean events. Over the past 50 years, the ocean has absorbed more than 90% of the additional heat gained by the Earth system (Dong et al., 2020).

We conclude that, in March 2024, a severe MHW event was identified by the SiMCosta BA01 buoy, which stood out as the only such event recorded in the past five years. Severe MHW events are of great concern due to their potential devastating consequences for marine environments, possibly causing widespread loss of habitat-forming species such as algae and corals, altering species distribution and ecosystem structures. Moreover, the consequences of this event may extend beyond the marine environment, affecting food security and impacting the economic sector, with a particular emphasis on fishing, which relies on the health of marine ecosystems for its sustainability. The SiMCosta buoy data were crucial for identifying and understanding the characteristics of this MHW event. The measured data proved to be effective for analyzing the relationships between climate extremes and MHWs, especially on a local scale. Continuous SST monitoring enables a more accurate understanding, which is essential to manage and mitigate the impacts of these phenomena on marine ecosystems and related economic activities.

DATA AVAILABILITY STATEMENT

This study uses SiMCosta data, available for free download at <https://simcosta.furg.br/home>. It also incorporates data from the MarineHeatwaves group, accessible at <https://www.marineheatwaves.org/>.

SUPPLEMENTARY MATERIAL

There is no supplementary material.

FUNDING

This research was funded by National Council for Scientific and Technological Development (CNPq), processes numbers 380198/2024-0 and 409666/2022-0.

ACKNOWLEDGMENTS

We express our gratitude to the Brazilian Coastal Monitoring System (SiMCosta) team for providing crucial data, the marineheatwaves.org group for their tools and resources, and the National Council for Scientific and Technological Development (CNPq) for their financial support of the National Ocean Observation and Monitoring Network (ReNOMO).

AUTHOR CONTRIBUTIONS

B.A.O.D.: Conceptualization; Methodology; Writing – original draft; Writing – review & editing.

C.A.E.G.: Conceptualization; Resources; Supervision; Funding; Writing – review & editing.

CONFLICTS OF INTEREST

The authors declare there is no conflict of interest and no competing financial interests.

REFERENCES

- Amaya, D. J. & Foltz, G. R. 2014. Impacts of canonical and Modoki El Niño on tropical Atlantic SST. *Journal of Geophysical Research: Oceans*, 119(2), 777–789. DOI: <https://doi.org/10.1002/2013JC009476>
- Cai, W., McPhaden, M. J., Grimm, A. M., Rodrigues, R. R., Taschetto, A. S., Garreaud, R. D., Dewitte, B., Poveda, G., Ham, Y.-G., Santoso, A., Ng, B., Anderson, W., Wang, G., Geng, T., Jo, H.-S., Marengo, J. A., Alves, L. M., Osman, M., Li, S., Wu, L., Karamperidou, C., Takahashi, K. & Vera, C. 2020. Climate impacts of the El Niño–Southern Oscillation on South America. *Nature Reviews Earth & Environment*, 1(4), 215–231. DOI: <https://doi.org/10.1038/s43017-020-0040-3>
- Cheung, W. W. L. & Frölicher, T. L. 2020. Marine heatwaves exacerbate climate change impacts for fisheries in the northeast Pacific. *Scientific Reports*, 10(1), 6678. DOI: <https://doi.org/10.1038/s41598-020-63650-z>
- Chiang, J. C. H. & Vimont, D. J. 2004. Analogous Pacific and Atlantic Meridional Modes of Tropical Atmosphere–Ocean Variability*. *Journal of Climate*, 17(21), 4143–4158. DOI: <https://doi.org/10.1175/JCLI4953.1>
- Clark, N. E., Eber, L. E., Laurs, R. M., Renneer, J. A. & Saur, J. F. T. (1974). Heat exchange between ocean and atmosphere in the eastern North Pacific for

- 1961-71. Seattle, National Oceanic and Atmospheric Administration.
- Costa, N. V. & Rodrigues, R. R. 2021. Future Summer Marine Heatwaves in the Western South Atlantic. *Geophysical Research Letters*, 48(22), e2021GL094509. DOI: <https://doi.org/10.1029/2021GL094509>
- Dong, S., Lopez, H., Lee, S., Meinen, C. S., Goni, G. & Baringer, M. 2020. What Caused the Large-Scale Heat Deficit in the Subtropical South Atlantic Ocean During 2009–2012? *Geophysical Research Letters*, 47(11), e2020GL088206. DOI: <https://doi.org/10.1029/2020GL088206>
- Drumond, A., Marengo, J., Ambrizzi, T., Nieto, R., Moreira, L. & Gimeno, L. 2014. The role of the Amazon Basin moisture in the atmospheric branch of the hydrological cycle: a Lagrangian analysis. *Hydrology and Earth System Sciences*, 18(7), 2577–2598. DOI: <https://doi.org/10.5194/hess-18-2577-2014>
- Fairall, C. W., Bradley, E. F., Rogers, D. P., Edson, J. B. & Young, G. S. 1996. Bulk parameterization of air-sea fluxes for Tropical Ocean-Global Atmosphere Coupled-Ocean Atmosphere Response Experiment. *Journal of Geophysical Research: Oceans*, 101(C2), 3747–3764. DOI: <https://doi.org/10.1029/95JC03205>
- Ferreira, L. C. L., Grillo, A. C., Repinaldo Filho, F. P. M., Souza, F. N. R. & Longo, G. O. 2021. Different responses of massive and branching corals to a major heatwave at the largest and richest reef complex in South Atlantic. *Marine Biology*, 168(5), 54. DOI: <https://doi.org/10.1007/s00227-021-03863-6>
- Foltz, G. R., McPhaden, M. J. & Lumpkin, R. 2012. A Strong Atlantic Meridional Mode Event in 2009: The Role of Mixed Layer Dynamics*. *Journal of Climate*, 25(1), 363–380. DOI: <https://doi.org/10.1175/JCLI-D-11-00150.1>
- Fung, I. Y., Harrison, D. E. & Lacis, A. A. 1984. On the variability of the net longwave radiation at the ocean surface. *Reviews of Geophysics*, 22(2), 177–193. DOI: <https://doi.org/10.1029/RG022i002p00177>
- Garfinkel, C. I. & Hartmann, D. L. 2010. Influence of the quasi-biennial oscillation on the North Pacific and El Niño teleconnections. *Journal of Geophysical Research: Atmospheres*, 115(D20), 2010JD014181. DOI: <https://doi.org/10.1029/2010JD014181>
- Giannini, A., Saravanan, R. & Chang, P. 2004. The preconditioning role of Tropical Atlantic Variability in the development of the ENSO teleconnection: implications for the prediction of Nordeste rainfall. *Climate Dynamics*, 22(8), 839–855. DOI: <https://doi.org/10.1007/s00382-004-0420-2>
- González Hernández, M. M., León, C. J., García, C. & Lam-González, Y. E. 2023. Assessing the climate-related risk of marine biodiversity degradation for coastal and marine tourism. *Ocean & Coastal Management*, 232, 106436. DOI: <https://doi.org/10.1016/j.ocecoaman.2022.106436>
- Grimm, A. M., Barros, V. R. & Doyle, M. E. 2000. Climate Variability in Southern South America Associated with El Niño and La Niña Events. *Journal of Climate*, 35–58. DOI: [https://doi.org/10.1175/1520-0442\(2000\)013<0035:CVISSA>2.0.CO;2](https://doi.org/10.1175/1520-0442(2000)013<0035:CVISSA>2.0.CO;2)
- Hobday, A. J., Alexander, L. V., Perkins, S. E., Smale, D. A., Straub, S. C., Oliver, E. C. J., Benthuyssen, J. A., Burrows, M. T., Donat, M. G., Feng, M., Holbrook, N. J., Moore, P. J., Scannell, H. A., Sen Gupta, A. & Wernberg, T. 2016. A hierarchical approach to defining marine heatwaves. *Progress in Oceanography*, 141, 227–238. DOI: <https://doi.org/10.1016/j.pocean.2015.12.014>
- Hobday, A. J., Oliver, E. C. J., Gupta, A. S., Benthuyssen, J. A., Burrows, M. T., Donat, M. G., Holbrook, N. J., Moore, P. J., Thomsen, M. S., Wernberg, T. & Smale, D. A. 2018. Categorizing and Naming MARINE HEATWAVES. *Oceanography*, 31(2), 162–173. Accessed: <https://www.jstor.org/stable/26542662>
- Hoerling, M. P., Kumar, A. & Zhong, M. 1997. El Niño, La Niña, and the Nonlinearity of Their Teleconnections. *Journal of Climate*, 10(8), 1769–1786. DOI: [https://doi.org/10.1175/1520-0442\(1997\)010<1769:ENOLNA>2.0.CO;2](https://doi.org/10.1175/1520-0442(1997)010<1769:ENOLNA>2.0.CO;2)
- Hsiung, J. 1985. Estimates of Global Oceanic Meridional Heat Transport. *Journal of Physical Oceanography*, 15(11), 1405–1413. DOI: [https://doi.org/10.1175/1520-0485\(1985\)015<1405:EEOGMH>2.0.CO;2](https://doi.org/10.1175/1520-0485(1985)015<1405:EEOGMH>2.0.CO;2)
- Hughes, T. P., Kerry, J. T. & Simpson, T. 2018. Large-scale bleaching of corals on the Great Barrier Reef. *Ecology*, 99(2), 501–501. DOI: <https://doi.org/10.1002/ecy.2092>
- Li, Y., Xie, S., Lian, T., Zhang, G., Feng, J., Ma, J., Peng, Q., Wang, W., Hou, Y. & Li, X. 2023. Interannual Variability of Regional Hadley Circulation and El Niño Interaction. *Geophysical Research Letters*, 50(4), e2022GL102016. DOI: <https://doi.org/10.1029/2022GL102016>
- Morgan, K. M., Perry, C. T., Johnson, J. A. & Smithers, S. G. 2017. Nearshore Turbid-Zone Corals Exhibit High Bleaching Tolerance on the Great Barrier Reef Following the 2016 Ocean Warming Event. *Frontiers in Marine Science*, 4, 224. DOI: <https://doi.org/10.3389/fmars.2017.00224>
- Medeiros, F. J. & Oliveira, C. P. 2021. Dynamical Aspects of the Recent Strong El Niño Events and Its Climate Impacts in Northeast Brazil. *Pure and Applied Geophysics*, 178(6), 2315–2332. DOI: <https://doi.org/10.1007/s00024-021-02758-3>
- Neelin, J. D., Chou, C. & Su, H. 2003. Tropical drought regions in global warming and El Niño teleconnections. *Geophysical Research Letters*, 30(24), 2003GL018625. DOI: <https://doi.org/10.1029/2003GL018625>
- Nobre, P. & Srulka, J. 1996. Variations of Sea Surface Temperature, Wind Stress, and Rainfall over the Tropical Atlantic and South America. *Journal of Climate*, 9(10), 2464–2479. DOI: [https://doi.org/10.1175/1520-0442\(1996\)009<2464:VOSSTW>2.0.CO;2](https://doi.org/10.1175/1520-0442(1996)009<2464:VOSSTW>2.0.CO;2)
- Oliver, E. C. J., Donat, M. G., Burrows, M. T., Moore, P. J., Smale, D. A., Alexander, L. V., Benthuyssen, J. A., Feng, M., Sen Gupta, A., Hobday, A. J., Holbrook, N. J., Perkins-Kirkpatrick, S. E., Scannell, H. A., Straub, S. C. & Wernberg, T. 2018. Longer and more frequent marine heatwaves over the past century. *Nature Communications*, 9(1), 1324. DOI: <https://doi.org/10.1038/s41467-018-03732-9>
- Reed, R. K. 1977. On Estimating Insolation over the Ocean. *Journal of Physical Oceanography*, 7(3), 482–485. DOI: [https://doi.org/10.1175/1520-0485\(1977\)007<0482:OEIOTO>2.0.CO;2](https://doi.org/10.1175/1520-0485(1977)007<0482:OEIOTO>2.0.CO;2)
- Roberts, S. D., Van Ruth, P. D., Wilkinson, C., Bastianello, S. S. & Bansemer, M. S. 2019. Marine Heatwave,

- Harmful Algae Blooms and an Extensive Fish Kill Event During 2013 in South Australia. *Frontiers in Marine Science*, 6, 610. DOI: <https://doi.org/10.3389/fmars.2019.00610>
- Rodrigues, R. R., Haarsma, R. J., Campos, E. J. D. & Ambrizzi, T. 2011. The Impacts of Inter–El Niño Variability on the Tropical Atlantic and Northeast Brazil Climate. *Journal of Climate*, 24(13), 3402–3422. DOI: <https://doi.org/10.1175/2011JCLI3983.1>
- Rodrigues, R. R. & McPhaden, M. J. 2014. Why did the 2011–2012 La Niña cause a severe drought in the Brazilian Northeast? *Geophysical Research Letters*, 41(3), 1012–1018. DOI: <https://doi.org/10.1002/2013GL058703>
- Schlegel, R. W. (2020). Marine heatwave tracker. See <http://www.marineheatwaves.org/tracker>.
- Smith, K. E., Burrows, M. T., Hobday, A. J., Sen Gupta, A., Moore, P. J., Thomsen, M., Wernberg, T. & Smale, D. A. 2021. Socioeconomic impacts of marine heatwaves: Global issues and opportunities. *Science*, 374(6566), eabj3593. DOI: <https://doi.org/10.1126/science.abj3593>
- Taschetto, A. S., Ummenhofer, C. C., Stuecker, M. F., Dommenges, D., Ashok, K., Rodrigues, R. R. & Yeh, S. 2020. ENSO Atmospheric Teleconnections. In: McPhaden, M. J., Santoso, A., & Cai, W. (Eds). *Geophysical Monograph Series* (pp. 309–335). Wiley.
- Tedeschi, R. G., Grimm, A. M. & Cavalcanti, I. F. A. 2015. Influence of Central and East ENSO on extreme events of precipitation in South America during austral spring and summer. *International Journal of Climatology*, 35(8), 2045–2064. DOI: <https://doi.org/10.1002/joc.4106>
- Vogt, L., Burger, F. A., Griffies, S. M. & Frölicher, T. L. 2022. Local Drivers of Marine Heatwaves: A Global Analysis With an Earth System Model. *Frontiers in Climate*, 4, 847995. DOI: <https://doi.org/10.3389/fclim.2022.847995>
- Yang, Q., Cokelet, E. D., Stabeno, P. J., Li, L., Hollowed, A. B., Palsson, W. A., Bond, N. A. & Barbeaux, S. J. 2019. How “The Blob” affected groundfish distributions in the Gulf of Alaska. *Fisheries Oceanography*, 28(4), 434–453. DOI: <https://doi.org/10.1111/fog.12422>